Contribution of Ionization and Lipophilicity to Drug Binding to Albumin: A Preliminary Step toward Biodistribution Prediction

Giuseppe Ermondi, Miriam Lorenti, and Giulia Caron*

Dipartimento di Scienza e Tecnologia del Farmaco, Università di Torino, Via P. Giuria 9, I-10125 Torino, Italy

Received January 5, 2004

Understanding the molecular mechanisms governing albumin binding is a major challenge in absorption−distribution−metabolism−excretion prediction. To gain insight into this complex field, an ultracentrifugation method to measure the drug fraction bound to bovine serum albumin [%B(DAB)] is presented. The second part of the study shows the dependence of the experimental binding parameter on ionization and lipophilicity descriptors (pK_a and log $D_{oct}^{7.4}$ for a series of 14 structurally diverse drugs. Finally, a docking strategy is used to rationalize the findings; the results confirm the mostly nonspecific nature of the interaction of albumin with neutral ligands.

Introduction

The need to screen absorption−distribution−metabolism−excretion (ADME) characteristics at a very early stage of drug development is rapidly growing. Protein binding influences many pharmacokinetic characteristics[1] and may involve one or several macromolecules. The simplest situation is that in which only one protein is involved. The most frequent case concerns the drug−albumin complex, since albumin is the most abundant plasma protein, at around 0.6 mM (about 40 g/1000 mL, 4%).[2] Because of its abundance, it is reasonable to assume that the binding strength of a given drug to serum albumin and thus free drug exposure is fundamental to understanding therapeutic responses.[3]

Human serum albumin (HSA), a 585 residue protein, contains three homologous domains (labeled I−III), each consisting of two subdomains (A and B) that share common structural elements. Recent studies have also reported the crystal structures of HSA with some of its ligands: fatty acids,[4,5] warfarin,[6] propofol, and halothane.[7]

A literature overview indicates three major limitations of plasma protein binding studies: (i) results obtained in different laboratories are not often comparable;[8,9] (ii) quantitative structure−pharmacokinetic relationships (QSPkR) in the field are often limited to structurally related classes of compounds;[10−17] and (iii) despite the high number of powerful molecular modeling tools available today, there is in practice only one report of plasma protein binding.[18]

This study aims to obtain information on drug albumin binding mechanisms by using a strategy based on the combination of experimental data and molecular modeling tools, namely, conformational analysis and docking strategies. The paper is divided into three parts: first, an ultracentrifugation method (ultracentrifugation is a widely used technique to measure binding[19,20]) was set up to determine drug binding to bovine serum albumin (BSA) experimentally. The method was applied to a set of structurally diverse drugs (Figure 1) with well-dispersed lipophilicity and ionization characteristics. Second, the relationships between albumin binding and log $D^{7.4}$ (the logarithm of the distribution coefficient D at pH 7.4 in octanol/water, traditionally assumed to dominate binding to albumin[21]) were analyzed following a recent approach to lipophilicity;[22] in addition, a careful check of the literature was made, and the dependence of reliable binding descriptors and lipophilicity is discussed for the same set of compounds. Finally, a link between experimental results and molecular interaction mechanisms was sought. A search in the Protein Data Bank[23] furnished a number of results for the HSA query. In particular, in Bhattacharya et al.,[4] the high resolution of the crystallographic determination (2.2 Å) enabled the position of two propofol molecules to be determined unambiguously. Knowing the crystal structure of the complex and using the MOE (molecular operating environment) program package,[24] a molecular docking strategy was set up that was able to confirm the QSPkR results. Overall, the study contributes to our understanding of the molecular forces involved in drug−albumin interaction and thus to the prediction of biodistribution properties.

Results and Discussion

Data Set of Compounds. The goal of our study is to have preliminary but well-founded insights into the role of ionization and lipophilicity in albumin binding, by working on a small but significant data set (Figure 1) for which high precision experimental determinations have been performed. A careful examination of serum protein binding data reported in the literature shows that results obtained in different laboratories are not often comparable, due to failure to describe the experimental conditions in proper detail, frequently combined with insufficient methodological accuracy, and inappropriate choice of descriptors.

Principal component analysis (PCA) was used to investigate the heterogeneity of the working data set.[25] Figure 2 gives the scores of the first two principal components (t1 and t2), which describe 71% of the diversity in the descriptors space. The data set was found to cover all four quadrants of the PCA plot, showing to be heterogeneous and thus significant.

* To whom correspondence should be addressed. Tel: +390116707282. Fax: +390116707687. E-mail: giulia.caron@unito.it.

10.1021/jm040760a CCC: $27.50
Published on Web 07/02/2004

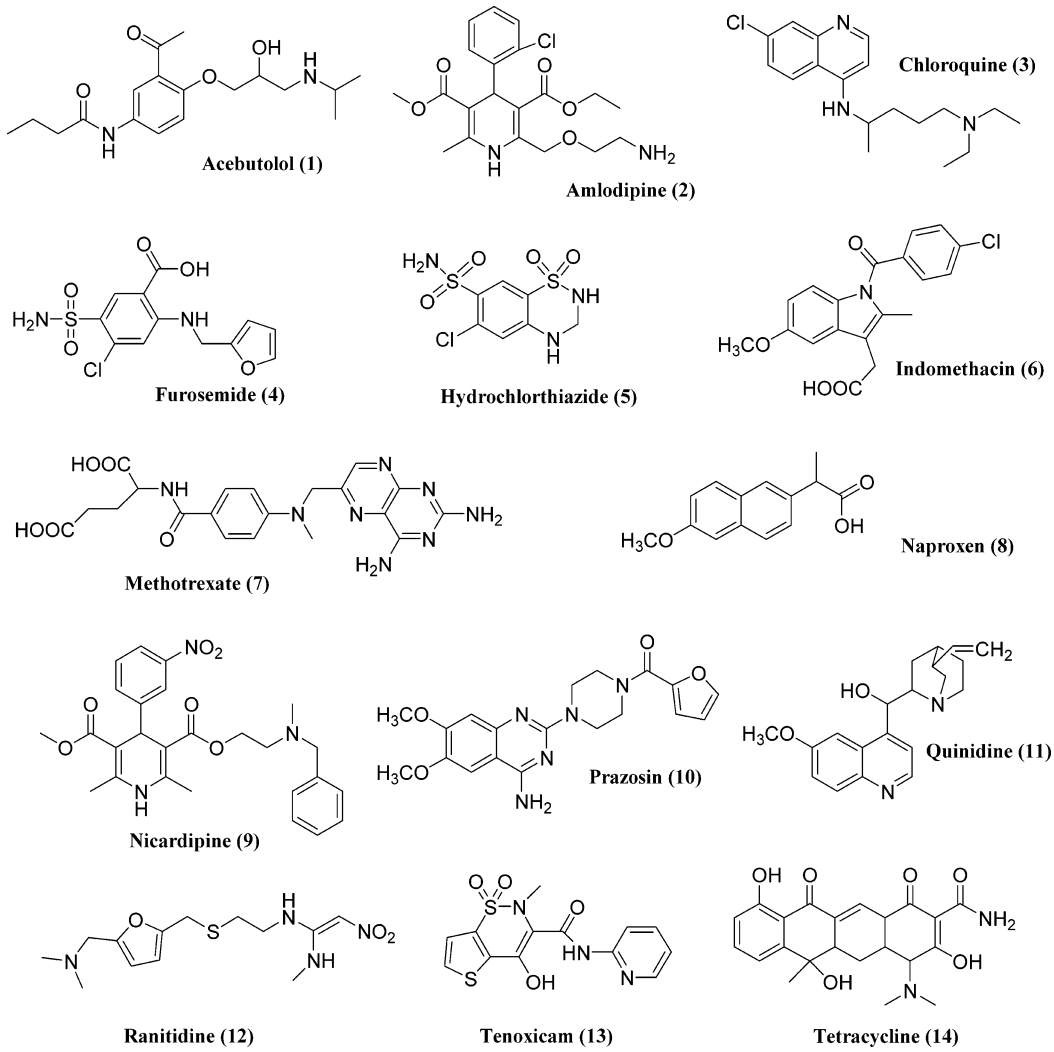

Figure 1. Chemical structures of compounds under study.

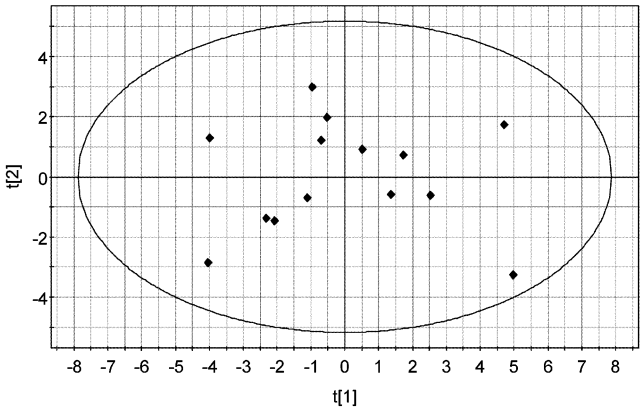

Figure 2. Heterogeneity of the selected data set investigated by PCA.

Determination of Albumin Binding. To obtain binding data under rigorous conditions, the mathematical equations associated with the biological phenomenon must be known. Equation 1 (obtained from the law of mass action) is commonly used[15] to quantitatively describe protein binding.

$$C_B = \frac{n_{A1} \cdot P_t \cdot K_{A1} \cdot C_U}{1 + K_{A1} \cdot C_U} + n_{A2} \cdot P_t \cdot K_{A2} \cdot C_U \quad (1)$$

where C_B is the concentration (mM) of the bound fraction, K_{A1} (K_{A2}) is the first (second) association constant expressed in mM^{-1}, n_{A1} (n_{A2}) is the number of binding sites per protein molecule associated to K_{A1} (K_{A2}), P_t is the total protein concentration, and C_U is the concentration (mM) of the unbound fraction. In Figure 3A, eq 1 is represented for methohexital based on the experimental data reported in Girard et al.[15]

For the sake of clarity, the second term of eq 1, which refers to a nonsaturable class of sites of low affinity and is associated with experimental conditions far from physiological values, can reasonably be neglected.[9] Equation 1 is thus simplified to eq 2 (rectangular hyperbola)

$$C_B = \frac{n_{A1} \cdot P_t \cdot K_{A1} \cdot C_U}{1 + K_{A1} \cdot C_U} \quad (2)$$

Equation 2 is simulated (Figure 3B) for two generic compounds whose K_A values (due to the simplification, K_A is actually K_{A1}) represent, respectively, the lowest (1 mM^{-1}, continuous line) and highest (10^4 mM^{-1}, dotted line) values of a physiologically normal range,[8,19] P_t is 0.6 mM (human blood albumin concentration), and n_{A1} has been kept constant at 1.

Binding descriptors can be divided into two categories according to their capacity to describe the full binding

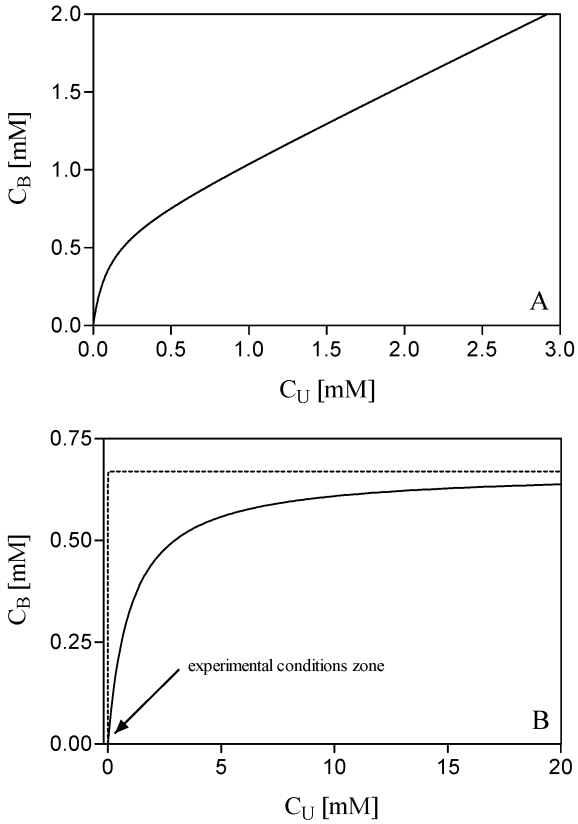

Figure 3. Simulation of binding curves. (A) Equation 1 in the case of methohexital. Experimental data (reported in ref 15): $n_{A1} = 1.01$, $K_{A1} = 11.2$ mM^{-1}, $n_{A2}K_{A2} = 0.81$ mM^{-1}, $P_t = 0.6$ mM. (B) Equation 2 was simulated for two generic compounds whose K_A (K_A means K_{A1}) represents, respectively, the lower (1 mM^{-1}) and the higher (10^4 mM^{-1}) values; P_t is 0.6 mM and $n_{A1} = 1$.

curve (Figure 3) or a single point: binding constants (K_A) and percentages of bound compound (%B), respectively. K_A (and its reciprocal K_D) is a constant peculiar to each individual drug. K_A values obtained in different laboratories are often not comparable[8] mainly because of the different fitting procedures adopted. %B depends on drug and protein concentrations, but it is quicker and easier to obtain than K_A, provided that a rational and accurate method is set up. It is therefore reasonable to take %B as the preferred descriptor for the very early screening stage of drug discovery. It should be remembered that because of their definitions, percentage data cannot legitimately be converted to the equivalent binding affinities, although the reverse procedure is legitimate.

Before choosing experimental conditions to measure %B, it must be kept in mind that the binding mode between drugs and albumin can be either saturable (first term of eq 1 and first part of Figure 3A) or nonsaturable (second term of eq 1 and second part of Figure 3A).[26] Which set of conditions should be chosen to determine %B? We selected conditions as close as possible to the values normally occurring in physiological conditions. For albumin, the normal concentration (0.6 mM) was adopted. The drug concentration (0.02 mM) was chosen taking into account the following factors: aqueous solubility at pH 7.4, UV detection, and therapeutic range of activity (a good lead compound should be active at a concentration of 10 μM or below[27]). This situation corresponds to the extreme lower left of the curves reported in Figure 3 and thus demonstrates that for a reasonable normal K_{A1} range (see above), saturable conditions should be selected.

The 14 common drugs constituting our data set (Figure 1) were submitted to albumin binding tests. Numerical results (Table 1) indicate that the percentage of BSA binding [%B(DAB)] ranges from 0 to 93% and that, as expected, acids bind more strongly to albumin than do neutral compounds, which in turn bind more strongly than bases. To a first approximation, it may therefore be said that a positive charge is detrimental to albumin binding, while a negative charge is favorable.

Ionization and Lipophilicity Properties. The experimental pK_a values of the compounds studied are listed in Table 1. Eleven of the 14 drugs have simple ionization profiles: furosemide, indomethacin, and naproxen are anions at pH 7.4; acebutolol, amlodipine, chloroquine, quinidine, and ranitidine are cations at pH 7.4; and hydrochlorthiazide, nicardipine, and prazosin are less than 90% ionized at pH 7.4 and, thus, in this study were considered neutral compounds at physiological pH. Tenoxicam has been described in detail by Tsai et al.[28] as an anion at pH 7.4.

Table 1. %B(DAB) for the Homogeneous Set of Compounds

drug	%B(DAB) ± SD[a]	N[b]	pK_a[c]	species[d]	log $D^{7.4}$[e]
acebutolol (**1**)	0.0 ± 5.0	5	9.52[f]	c	0.04[f]
amlodipine (**2**)	65.4 ± 2.0	10	9.03[g]	c	1.55[g]
chloroquine (**3**)	8.7 ± 1.5	4	8.10, 9.94	c	1.23[h]
furosemide (**4**)	87.2 ± 2.0	5	3.52, 10.63[i]	a	−1.03[h]
hydrochlorthiazide (**5**)	50.8 ± 3.2	5	8.76, 9.95[i]	n	−0.19[h]
indomethacin (**6**)	91.1 ± 2.0	5	4.5[f]	a	1.61[j]
methotrexate (**7**)	49.9 ± 2.1	4	3.76, 4.83, 5.60	n	−2.52
naproxen (**8**)	>95	4	4.18[j]	a	0.06[g]
nicardipine (**9**)	93.4 ± 5.9	5	7.17[g]	n	4.25[g]
prazosin (**10**)	46.4 ± 2.5	6	6.5[g]	n	0.79[g]
quinidine (**11**)	27.8 ± 1.5	5	4.46, 8.52[f]	c	2.41[f]
ranitidine (**12**)	3.9 ± 0.4	5	8.48[g]	c	−0.48[g]
tenoxicam (**13**)	89.6 ± 0.9	5	4.95[l]	a	−0.32[k]
tetracycline (**14**)	35.5 ± 1.2	5	3.3, 7.7, 9.5	n	−1.37

[a] Experimentally determined as described in the experimental part. [b] Number of the experiments. [c] Minus the logarithm of the ionization constants, taken from ref 33 unless indicated otherwise. [d] Dominant (>90%) species at physiological pH: n = neutral or ampholite, a = anion, and c = cation. [e] Logarithm of the distribution coefficient at pH 7.4 taken from ref 69 unless indicated otherwise. [f] Taken from ref 70. [g] Potentiometric determination obtained as described in ref 54. [h] log P taken from ref 69; correspondent log D calculated as described in the Experimental Section. [i] Taken from ref 71. [j] log P taken from ref 36; correspondent log D calculated as described in the Experimental Section. [k] Taken from ref 72.

For the ampholytes (ampholyte = compound bearing an acidic and a basic group[29]) tetracycline and methotrexate, there is no clear attribution of the pK_a values on the ionization centers; thus, identification of the electrical species predominating at physiological pH is not evident. In addition, controversial reports appeared in the literature[30,31] with regard to tetracycline. To gain more information on these compounds, ADME Boxes software[32] was used to predict their pK_a values and ionization profiles. For **14**, the zwitterionic species clearly dominates at pH 7.4; thus, **14** is considered neutral. For **7**,[33] the predicted pK_a values are not very convincing, mainly because of the presence of intramolecular effects; thus, because of its ampholitic nature, **7** is only neutral into a first approximation. However, investigation of the complex ionization profile of methotrexate is beyond the scope of this study.

Both the concepts[22,34] and the measurements of lipophilicity[35−37] have evolved considerably in recent years. Among the plethora of available descriptors,[22,37,38] the logarithm of the distribution coefficient in the *n*-octanol/water system at pH 7.4 (log $D_{oct}^{7.4}$ or simply log $D^{7.4}$) is the most convenient to use here, because it takes ionization into account and a number of computational tools exist that serve to check it. Lipophilicity values are given in Table 1: log $D^{7.4}$ data range from −2.52 (methotrexate) to 4.25 (nicardipine).

Relations between Binding and Lipophilicity (QSPkR). To date, QSPkR studies on protein binding have shown ionization[39] and lipophilicity[1,8,11,17,21,39−41] to play fundamental governing roles, although some doubts has been thrown on this traditional assumption.[9]

%B(DAB) vs Ionization and Lipophilicity Descriptors. A discrete three levels variable I ($I = -1$ for acids, $I = +1$ for bases, and $I = 0$ for neutral compounds) together with log $D^{7.4}$ (logarithm of distribution coefficient at pH 7.4) was used as an independent variable in a MLR run where %B(DAB) was the dependent variable (eq 3).

$$\%B(DAB) = 7.67(\pm 2.75) \cdot \log D^{7.4} - 37.63(\pm 6.11) \cdot I + 52.24(\pm 4.81) \quad (3)$$

where $n = 13$, $s = 16.57$, $r^2 = 0.801$, and $F = 20$.

In this and the following equations, 95% confidence limits are given in round brackets, n is the number of compounds, s is the standard deviation, r^2 is the squared correlation coefficient, and F is the Fischer test. The plot of the residuals (not shown) indicates that amlodipine alone is poorly predicted by this equation.

Despite its limited statistical significance, eq 3 predicts %B(DAB) reasonably well for pregnenolone (85%, log $D^{7.4} = 4.22$) and testosterone (76%, log $D^{7.4} = 3.13$) taking values reported by Fischer et al.[42] (80 and 60%, respectively); the same may also be said for phenytoin (log $D^{7.4} = 2.47$; 81% is the experimental value reported in ref 43; 71% is the calculated result). Equation 3 also predicts a value of about 37% for imipramine (log $D^{7.4} = 3.0$), in excellent agreement with the 35% reported in the literature.[44] Pregnenolone, testosterone, phenytoin, and imipramine were selected to verify the predictive power of eq 3 because the original references unambiguously report experimental details and numerical results.

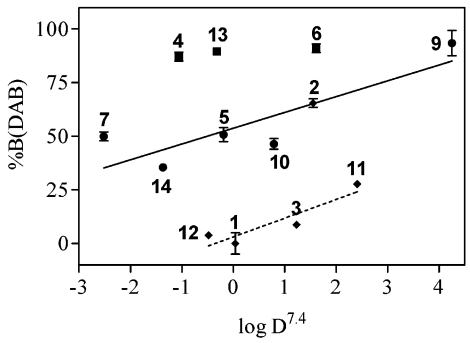

Figure 4. Plot of albumin binding data [(%B(DAB) with SD] and lipophilicity (log $D^{7.4}$); heterogeneous series of drugs: bases (◆), neutral compounds and ampholites (●), and acids (■). Linear relationships obtained for neutral and basic compounds are also reported; see text for comments.

The relationship between protein binding and lipophilicity was graphically investigated for the data set depicted in Figure 1. Figure 4 plots %B(DAB) vs log $D^{7.4}$. According to eq 3, the compounds are clearly separated by their I values: acids are in the upper part of the plot, bases are in the lower part, and neutral drugs are in the middle part.

Increasing lipophilicity appears to have almost no impact on the binding of acids with BSA as also deduced from eq 3. Furosemide **4** is a hydrophilic compound (log $D = -1.06$) but is as strongly bound to BSA as indomethacin **6** (log $D = 1.61$). The value for naproxen could not be determined precisely but is in line with other acidic drugs.

Neutral compounds behave differently from acids; an increase in lipophilicity corresponds to an increase in binding percentage as shown by eq 4.

$$\%B(DAB) = 7.34(\pm 2.56) \cdot \log D^{7.4} + 53.79(\pm 5.96) \quad (4)$$

where $n = 5$, $s = 13.3$, $r^2 = 0.752$, and $F = 8$.

Albumin binding of bases (except for amlodipine; see below) is also governed by lipophilicity (eq 5).

$$\%B(DAB) = 8.71(\pm 2.77) \cdot \log D^{7.4} + 3.13(\pm 3.81) \quad (5)$$

where $n = 4$, $s = 6.19$, $r^2 = 0.83$, and $F = 10$.

A table has recently been published by Kratochwil et al.[9] containing albumin binding data for about 100 drugs (together with ionization and lipophilicity descriptors). It might be interesting to use eq 3 (and/or eqs 4 and 5) to predict these data, but unfortunately, the table has a number of drawbacks: (i) it is not correct to assume a priori that plasma protein binding occurs exclusively to albumin (e.g., the percentage of bound imipramine is 93% in Kratochwil et al.[9] whereas 35% is the true value for albumin binding as described in Weder et al.[44]), and conversion of percentage data to equivalent binding affinities should be avoided (see above); (ii) ref 79 reported in Kratochwil et al.[9] (from which most data in Kratochwil's table were extracted) is inaccessible to many scientists because of its limited availability; and (iii) it is not clear what electrical species dominates at physiological pH, and sometimes, the ionization nature of the compound is in error (i.e., phenylbutazone at pH 7.4 is an acid, not a neutral compound). Because of these limitations, we tested eq 3 on some selected compounds for which albumin binding is unambiguously reported

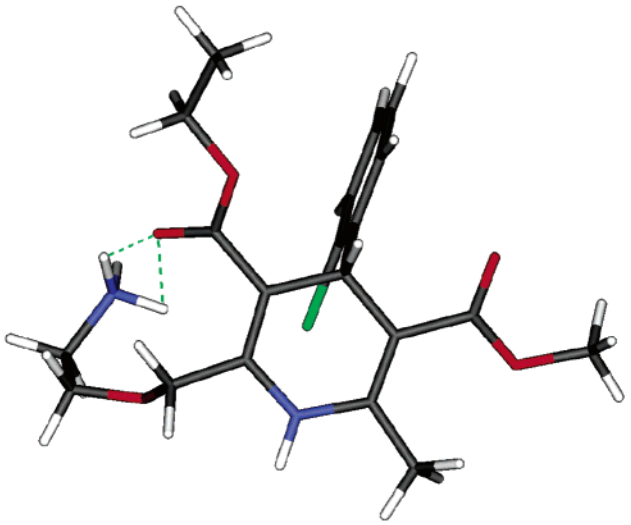

Figure 5. Most stable conformer of amlodipine obtained from QMD studies. Intramolecular HBs are shown.

in the original reference. Clearly, the validity of eq 3 must be checked with additional data.

Case of Amlodipine. Amlodipine bears a protonated amino group at physiological pH, but in the plot reported in Figure 4, it lies in the region of neutral compounds. Compound **2** is a dihydropyridine (DHP) calcium antagonist[45] comparable in potency to nifedipine but endowed with 100% oral availability and a long elimination half-life. Conformational analysis (quenched molecular dynamics, QMD) was used to unravel the reasons for its unexpectedly strong binding to BSA. The QMD results indicate that in all retained (15) conformers (see Experimental Section) the positive charge of the protonated amino group is always partially masked and that in many of them an intramolecular hydrogen bond (HB) is formed (Figure 5). Conversely, QMD of the neutral species revealed that in the absence of positive charge the contribution of folded conformers could be neglected. This finding would appear relevant to explaining the peculiar pharmacological behavior of **2**; hence, work is in progress to investigate the physicochemical behavior of amlodipine in greater depth.

Logarithm of the High-Performance Affinity Chromatography Binding Constant (log K_{hsa}') vs log $D^{7.4}$. High-performance affinity chromatography equipped with an immobilized HSA column has recently been proposed to determine albumin binding.[8] Plotting of chromatographic data taken from Colmenarejo et al.[8] (Table 2) and log $D^{7.4}$ (Figure 6) for compounds **1**−**14** showed no difference between neutral, basic, and acidic drugs, log K_{hsa}', being linearly related to lipophilicity by eq 6.

$$\log K_{hsa}' = 0.22(\pm 0.05) \cdot \log D^{7.4} - 0.03(\pm 0.07) \quad (6)$$

where $n = 10$, $s = 0.22$, $r^2 = 0.71$, and $F = 19$.

This finding might be caused by chromatographic artifacts: bound albumin is conformationally modified and is thus unable to respect its natural three-dimensional structure. In addition, as mentioned above, the protein/drug concentration ratio is the fundamental aspect to be taken into account when determining %B(DAB). This ratio cannot be determined in chromatographic methods; therefore, log K_{hsa}' is not a well-defined parameter. In other words, the two ways of obtaining BSA binding (ultracentrifugation and affinity chromatography) are not interchangeable, because they are governed by a different balance of intermolecular interactions. Interestingly, similar behavior has been seen in studies comparing lipophilicity in liposome/water systems with IAM column data.[46]

Table 2. Binding Data Taken from the Literature

drug	log K_{hsa}'[a]	%B(DPB)[b]
acebutolol (**1**)	−0.21	26.0
amlodipine (**2**)		98[c]
chloroquine (**3**)		61.0
furosemide (**4**)	−0.13	98.8
hydrochlorothiazide (**5**)	−0.42	64.0
indomethacin (**6**)	0.47	90.0
methotrexate (**7**)	−0.77	58.0
naproxen (**8**)	0.25	99.7
nicardipine (**9**)		99[d]
prazosin (**10**)	0.06	95.0
quinidine (**11**)	0.44	80.0
ranitidine (**12**)	−0.1	15.0
tenoxicam (**13**)		98.0[e]
tetracycline (**14**)	−0.08	65.0

[a] Data taken from ref 8. Log $K_{hsa}' = \log[(t - t_0)/t_0]$ in the conditions described in the text. [b] Percentage of drug bound in plasma [%B(DPB)]. Data taken from ref 40 unless indicated otherwise. [c] From ref 73. [d] From ref 74. [e] From ref 75.

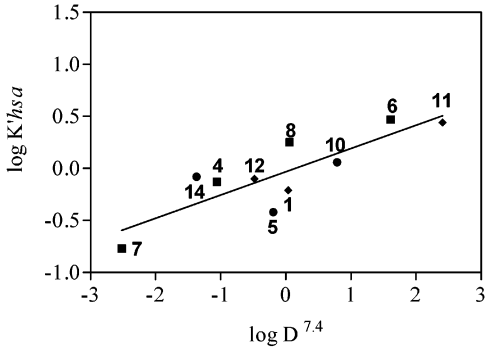

Figure 6. Linear relationships between log K_{hsa}' (literature data) and log $D^{7.4}$: bases (◆), neutral compounds and ampholites (●), and acids (■).

Percentage of Total Serum Protein Binding [%B(DPB)] vs log $D^{7.4}$. For the same 14 compounds, data concerning total plasma protein binding [%B(DPB), Table 2) were also collected and ranged from 15 to 99%. To a first approximation, we can assume that

$$\%B(DPB) = \%B(DAB) + \%B(AGP) + \%B(others) \quad (7)$$

where %B(DPB) and %B(DAB) are defined above, %B(AGP) is the percentage of drug bound to α1-glycoprotein, and %B(others) is the percentage of drug bound to the remaining plasma proteins (mainly lipoproteins).

The relationship between %B(DPB) and lipophilicity is illustrated in Figure 7A. Here again, acids are bound more strongly than neutral compounds, bases being the weakest (amlodipine again binds more than expected considering its cationic nature). For acids, there was no appreciable variation between %B(DAB) and %B(DPB) (Table 2), which confirms that albumin binding is the major factor determining acid binding to serum proteins. For acids, the contributions from %B(AGP) and %B(others) in eq 7 can be neglected.

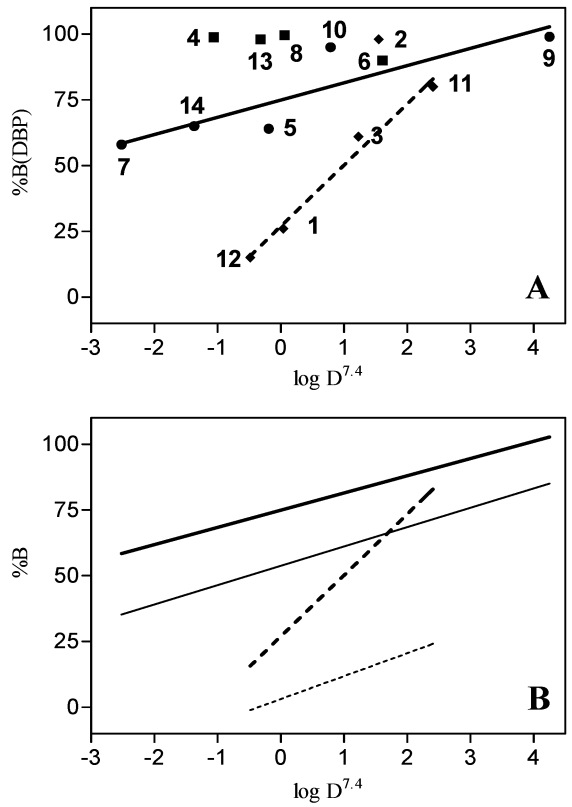

Figure 7. Relationships between %B(DPB) and %B(DAB) and lipophilicity. (A) %B(DPB) vs log $D^{7.4}$. (B) %B(DPB) (heavy lines: - - -, cations; —, neutral compounds) and %B(DAB) (thin lines: - - -, cations; —, neutral compounds) and log $D^{7.4}$.

For neutral drugs and bases, the dependence of %B(DPB) on lipophilicity is also linear (eqs 8 and 9, respectively, and Figure 7B).

$$\%B(DPB) = 6.54(\pm 2.03) \cdot \log D^{7.4} + 74.9(\pm 4.71) \quad (8)$$

where $n = 5$, $s = 10.5$, $r^2 = 0.776$, and $F = 10$.

$$\%B(DPB) = 23.2(\pm 2.07) \cdot \log D^{7.4} + 26.9(\pm 2.84) \quad (9)$$

where $n = 4$, $s = 4.62$, $r^2 = 0.984$, and $F = 126$.

Closer inspection of the slopes obtained plotting %B(DAB) and %B(DPB), respectively, as dependent variables (and log $D^{7.4}$ as an independent variable) indicates that in the presence of the whole serum proteins, an increase in slope occurs for cations but not for neutral compounds (Figure 7B). This could be in line with an additional contribution from AGP binding for bases; AGP indeed preferentially binds basic compounds.[2]

Interaction of Neutral Compounds with HSA Investigated by Molecular Modeling. The results obtained with eq 3 should be confirmed by a docking study. In particular, drugs with a high value of %B(DAB) should show better docking than those with low binding properties.

The crystal structure of HSA complexed with a number of endogenous[4,5] and exogenous ligands[6,7] has recently been reported. For this reason, in our computational study, we used HSA instead of BSA, for which no X-ray exists.

In this paper, docking results are discussed with the aid of preference maps (see the Experimental Section for details); briefly, this tool produces two grids, a green one that indicates the preferred hydrophobic contact regions and a red one that indicates the preferred polar contact regions. If the hydrophobic moieties of the ligand match the hydrophobic regions, the interaction is optimal (and likewise for the polar moieties and regions); conversely, if the hydrophobic groups of the ligands match the polar regions, or vice versa, the interaction is poor.

Validation of the Docking Procedure. With the aim of testing the docking procedure, propofol was subjected to the docking calculation. In the crystal structure,[7] propofol can bind in two sites: the first (PR1) is located in subdomain IIIA and is the site of highest affinity;[7] the second (PR2) is located in subdomain IIIB.

The docking procedure was successful in reproducing the binding mode of propofol found experimentally in both sites, but only PR1 is considered here.

Both the X-ray complex and the calculated complex (C4) reveal that the propofol molecule binds in an apolar pocket with the phenolic hydroxyl group, making a weak HB (3.5 Å) with the main chain carbonyl oxygen of Leu430 and with the aromatic ring of the molecule sandwiched between the side chain of Leu453 and Asn391. One of the two isopropyl groups makes numerous apolar contacts at one end of the pocket (mainly with Asn391, Val433, and Ala449), whereas the other is exposed at the aqueous entrance, although it makes contacts with several side chains (Arg410, Tyr411, and Leu430). The isopropyl group located at the mouth of the pocket is rotated by about 60° as compared to the X-ray solution to reduce contact with vicinal residues. The orientation C4 fits the preference maps closely as shown in Figure 8. From the docking calculations, a possible second binding mode (C1) was found at lower interaction energies (about 1 kcal/mol less that C4) but this orientation does not fit the preference maps well (data not shown) and thus was discarded.

Interaction Mode of Unionized Compounds with HSA as Deduced from Molecular Modeling. The modeling study was extended to three unionized compounds belonging to the data set (Figure 1), hydrochlorthiazide, nicardipine, and prazosin, assuming that their binding site is the same as that of propofol (PR1). This assumption is reasonable because it has been shown that the propofol binding site can also accommodate large molecules such as fatty acids.[7] In addition, locating the binding site of the neutral molecules in site IIIA is the most reasonable thing to do, because typically ligands in site IIA are bulky heterocyclic anions with the charge situated in a fairly central position of the molecule. This differentiates them from the ligands typical of site IIIA, which are generally aromatic and neutral; a charge, if present, is anionic and located more peripherically on the molecule.[19] Nevertheless, work is in progress to explore other sites in particular for acidic molecules.

A preliminary investigation made using Absolv[47] descriptors (according to Abraham's definition,[48] V_x is the molar McGowan's volume and α and β are the solute's H-bond donor acidity and H-bond acceptor basicity, respectively) reveals that hydrochlorthiazide is roughly the same size as propofol (V_x is 1.62 for propofol and 1.73 for **5**) but presents more hydrophilic

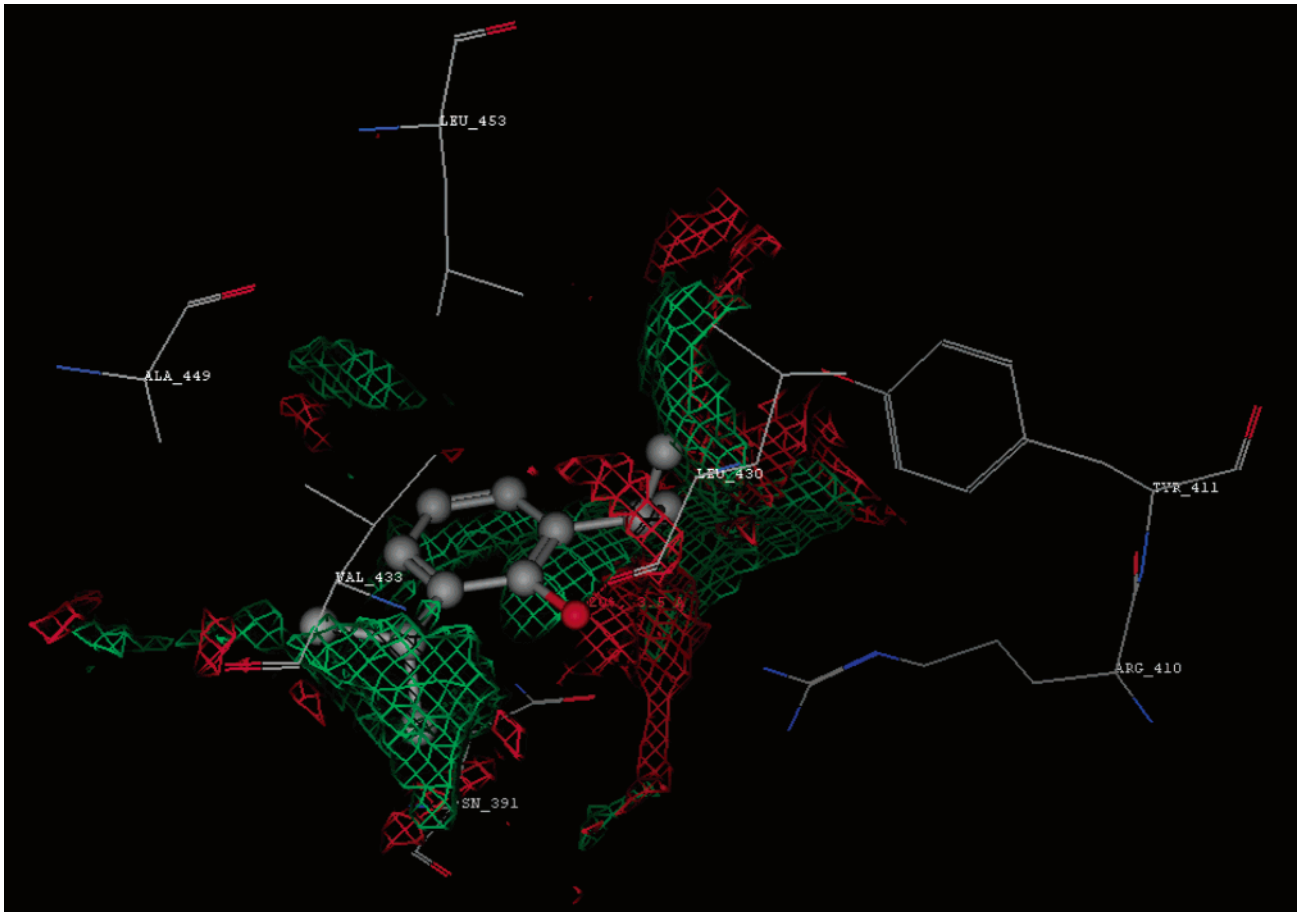

Figure 8. Propofol orientation C4 in the PR1 site. The hydrophilic preference map (90% probability) is in red, and the hydrophobic preference map (90% probability) is in green. Hydrogens were removed for clarity.

groups than propofol ($\alpha = 0.37$ and $\beta = 0.37$ for propofol and $\alpha = 1.46$ and $\beta = 1.72$ for hydrochlorthiazide); nicardipine is larger than propofol (V_x is 3.62), has a strong HB acceptor property ($\alpha = 0.31$ and $\beta = 2.20$), and presents a terminal hydrophobic group (phenyl); prazosin has roughly the same solvatochromic profile as nicardipine (V_x is 2.74, $\alpha = 0.24$, and $\beta = 2.22$). Conversely, BSA binding properties (Table 1) are similarly moderate for **5** and **10** and high for **9**. Application of the docking procedure to hydrochlorthiazide gives two orientations (C9 and C21) with a difference in interaction energy that is below 0.1 kcal/mol.

In orientation C9 (Figure 9A), the hydrochlorthiazide sulfonamide moiety is located at one end of the PR1 pocket, in proximity to Val433 and Ala449, whereas the 1,2,4-thiadiazine sulfoxide moiety forms a salt bridge with Arg412 (90% strength and 2.8 Å) and a HB with the hydroxyl group of Tyr411 (45% strength and 3.2 Å). The phenyl moiety is shifted with respect to propofol, and the sandwich between the side chains of Leu453 and Asn391 is less evident. The preference maps show a modest fit, and in particular, the sulfonamide group does not fit the maps.

In orientation C21 (Figure 9B), hydrochlorthiazide is flipped over with respect to C9; in this pose, the sulfonamide group forms two weak HBs with Tyr411 (13% strength and 3.6 Å) and with Ser489 (5% strength and 3.7 Å). The 1,2,4-thiadiazine sulfoxide moiety is located in the proximity of Val433 and Ala449 at the end of the PR1 pocket. The preference maps again show a controversial situation, the sulfonamide group having poor fit and only one of the oxygen atoms of the 1,2,4-thiadiazine sulfoxide group fitting well.

The results suggest that hydrochlorthiazide may be located at the propofol site PR1 with both favorable and unfavorable interactions. Preference maps cannot be used to determine the relative contribution of these contrasting effects, but it seems clear that hydrochlorthiazide cannot have a high percentage of albumin binding (about 51% according to Table 1).

The docking procedure applied to nicardipine gives only one relevant solution. Nicardipine is not entirely located in the pocket, its 1,4-DHP moiety being on the surface of albumin (Figure 9C). Only the lateral chain in three of the 1,4-DHP rings enters the pocket, with the phenyl ring occupying the same region as propofol. The 2-methyl group of 1,4-DHP is located in the proximity of Arg410 whereas the nitrophenyl moiety is located in the proximity of Leu387 and Gln390 out of the PR1 pocket. The lateral chain in three of the 1,4-DHP rings can form two HBs: the first at the surface of the protein between the ester group and the residue Asn391 (50% strength and 1.9 Å) and the second between the amino group and Tyr411 (3% strength and 3.7 Å). Finally, the phenyl ring fits less deeply than propofol in the PR1 pocket in the proximity of Phe403, Leu430, Leu407, and Asn391. The preference maps (Figure 9C) reveal a good fit for nicardipine; in particular, the 1,4-DHP ring and its 2-methyl group nicely fit at the HSA surface, and the phenyl ring in the PR1 pocket is located near a hydrophobic preferred region. The only aromatic nitro group has a poor fit.

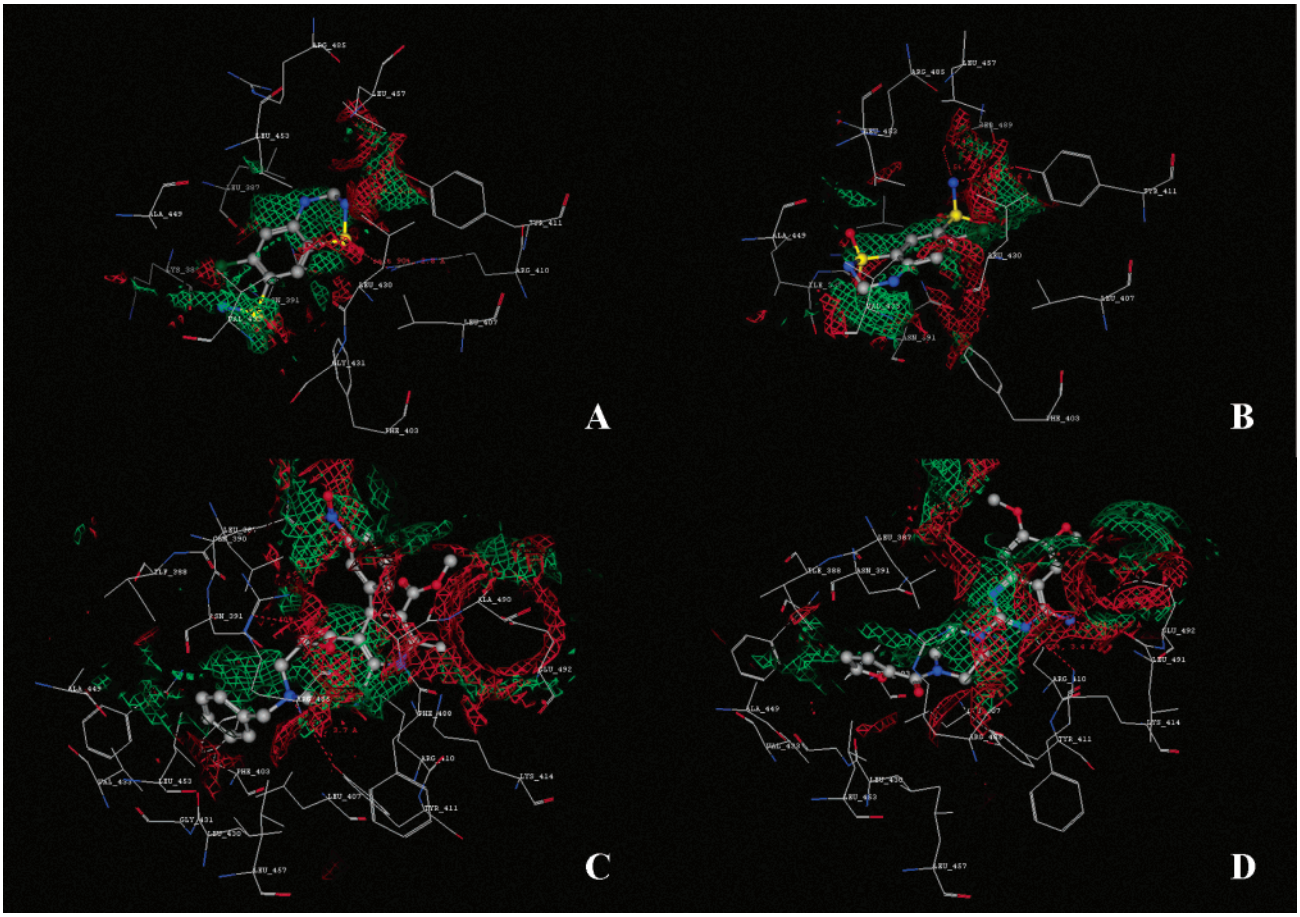

Figure 9. Docking results for the drugs investigated in the PR1 site. The hydrophilic preference map (90% probability) is in red, and the hydrophobic preference map (90% probability) is in green. Hydrogens were removed for clarity. (A) Hydrochlorthiazide orientation C9, (B) hydrochlorthiazide orientation C21, (C) nicardipine, and (D) prazosin.

Taken together, the docking results for nicardipine suggest that it is located in the propofol site PR1 and that mainly favorable interactions occur. It is thus reasonable to assume that nicardipine is strongly bound (about 93%, Table 1) to albumin.

A single orientation was also found for prazosin, with the quinazoline moiety located on the surface of albumin and the furanyl ring in the pocket occupied by propofol. The quinazoline moiety forms three HBs, the first with the carboxylic group of the side chain of Glu492 (26% strength and 3.4 Å), the second with the carboxylic group of Leu411, and the third with the amino group of Lys414 (Figure 9D). The two methoxy groups are located out of the pocket in the proximity of the side chain of Glu492 and Gln390. The piperazine moiety is located at the entrance of the PR1 pocket in the proximity of Arg410 and Tyr411. Finally, the furanyl ring is sandwiched between the side chain of Leu430 and Asn391 as in the case of the propofol phenyl ring. The results produced by the preference maps are controversial (Figure 9D): both bad (the methoxy groups) and good matches (the amino group) are present on the surface; the heterocyclic portion of quinazoline and the piperazine are located in a hydrophobic preferred contact region (green); thus, the nitrogen atoms do not fit well; finally, the furanyl ring fits worse than the phenyl group of nicardipine. As observed for hydrochlorthiazide, the docking results for prazosin also suggest that it can be located in the propofol site PR1, but both favorable and unfavorable interactions are present and determine a low binding (about 46% according to Table 1).

Taken together, the results achieved using this docking tool enable some general conclusions to be drawn as follows: (i) The PR1 site can act as a binding site for molecules larger than propofol provided that a portion of the molecule is able to occupy the propofol binding region (Figure 10), and (ii) HBs make a minimal contribution to binding.

Conclusion

At present, drug−albumin binding estimation is a major challenge in ADME prediction and thus in drug discovery. The search for a mathematical model to relate protein binding to molecular descriptors is ongoing, but some rules must be respected if reliable results are to be obtained. The quality of biological data (too often not comparable when obtained in different laboratories even for in vitro tests) represents the first bottleneck of the system. To overcome this difficulty, we designed a simple but rigorous method to determine the percentage of drug bound to albumin in physiological conditions for use at an early stage of drug discovery. It was applied to a significant data set of 14 well-known drugs.

Accuracy of drug descriptors is the second factor that can cause failure of a QSPkR study. In particular, there is great confusion surrounding the definition of acidic

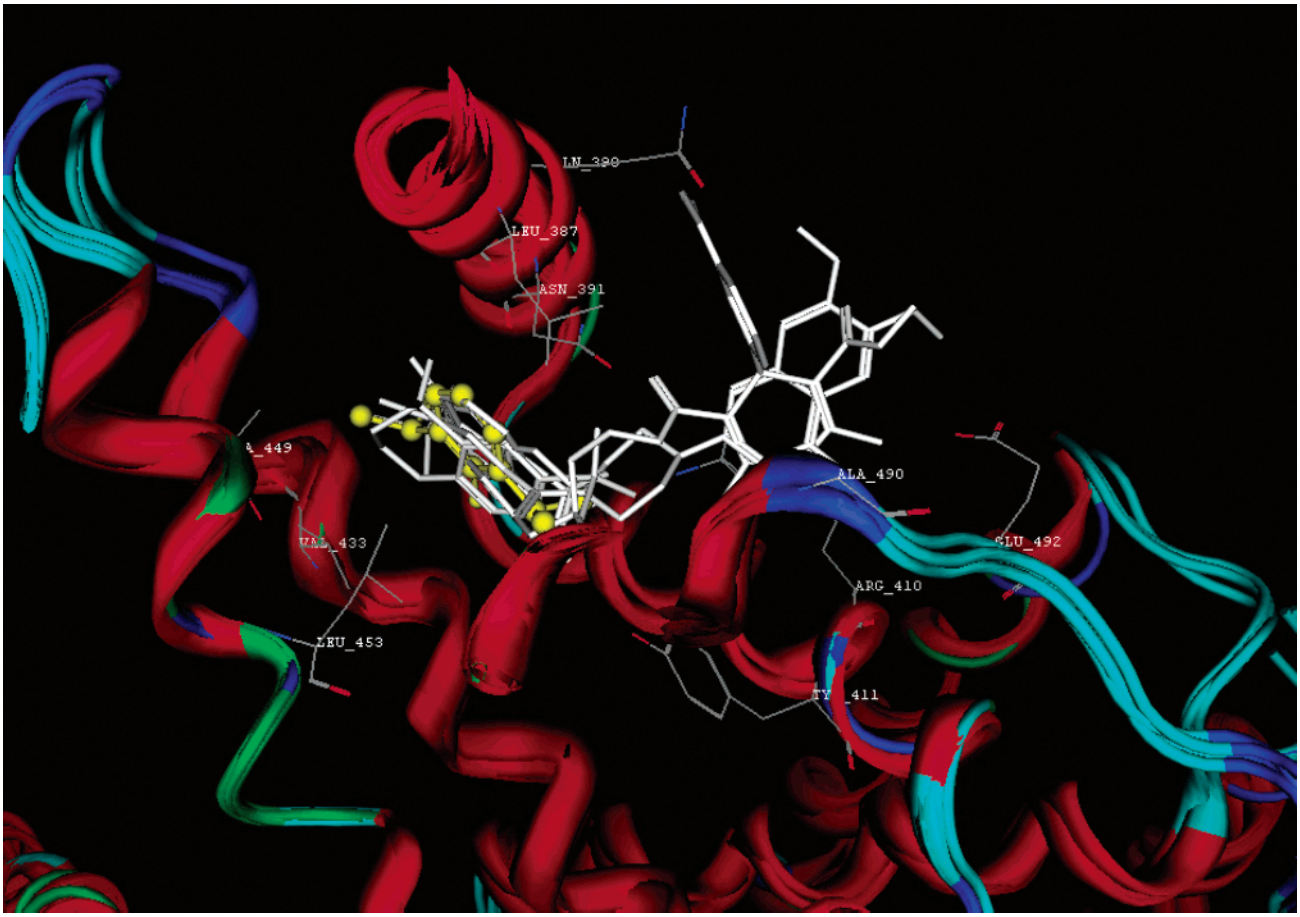

Figure 10. Final solutions of the docking procedure of the drugs investigated (in white) are superposed to the X-ray structure of propofol (in yellow).

and basic compounds in physiological conditions. We therefore set a general rule in this study to avoid misunderstanding about ionization, which is well-known to play a major role in protein binding, together with lipophilicity, which in turn was described by log $D^{7.4}$ (molecular descriptor including lipophilicity and ionization characteristics of compounds).

The results show that albumin binding depends mainly on ionization and second on lipophilicity. In fact, linear correlations between the percentage of drug bound [%B(DAB)] and log $D^{7.4}$ are reliable for neutral compounds and cations but not for anions, for which BSA binding is stronger probably because of supplementary electrostatic interactions. Taken together, these findings indicate that albumin binding depends on charge and lipophilicity. They are confirmed by docking simulations, which suggest that a substantial nonspecific interaction occurs between HSA and neutral drugs. The computational study also indicates that the PR1 site of propofol may be a binding site for molecules larger than propofol provided that a portion of the molecule can occupy the propofol binding region.

Considerable effort must still be devoted to extending these results to ionized compounds because the role of ligand charges in the interaction with albumin requires careful checking when setting up the docking tool. In addition, in particular in the case of acids, it will also be necessary to enlarge the number of experimental determinations.

Experimental Section

Reagents. Acebutolol hydrochloride (**1**), chloroquine diphosphate (**3**), furosemide (**4**), hydrochlorthiazide (**5**), indomethacin (**6**), methotrexate (**7**), naproxen (**8**), nicardipine hydrochloride (**9**), prazosin (**10**), quinidine (**11**), ranitidine (**12**), and tetracycline hydrochloride (**14**) are available commercially. Amlodipine (**2**) was extracted from Norvasc (Pfizer). Tenoxicam (**13**) was kindly offered to us by Dr. Pierre-Alain Carrupt (University of Lausanne, CH). The racemate of chiral drugs was always used.

BSA from Sigma-Aldrich (Milan, Italy), catalog number A7030, lyophilized powder minimum 98% (electrophoresis), was used. It is standard practice to use BSA for in vitro applications; HSA is employed only when a human protein is specifically required.[19]

PCA Analysis. All molecular descriptors were calculated using Dragon software[49] except for CLOGP and %B(DPB) (data from ref 40) and used as input matrix. The input matrix consisted of the following variables: MW = molecular weight; n_{AT} = number of atoms; n_{SK} = number of non-H atoms; n_{BT} = number of bonds; n_{BO} = number of non-H bonds; R_{BN} = number of rotatable bonds; n_{AB} = number of aromatic bonds; n_H = number of hydrogen atoms; n_C = number of carbon atoms; n_N = number of nitrogen atoms; n_O = number of oxygen atoms; n_{HDon} = number of donor atoms for H-bonds; n_{HAcc} = number of acceptor atom for H-bonds; and PSA = fragment-based polar surface area.

Ultracentrifugation Methodology. UV spectra and aqueous solubility of compounds were checked before performing experiments; the experimental determination of %B(DAB) for propofol was thus avoided because of its almost complete aqueous insolubility. The concentration of the BSA solution (solution A) was 4 g/100 mL in a phosphate buffer (0.0167 M) + 0.15 M KCl, pH 7.4.[19] To avoid foaming, the buffer solution

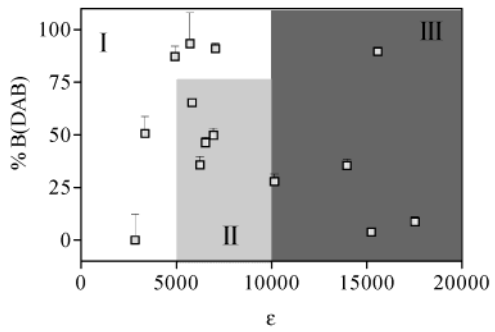

Figure 11. Experimental error of the method: plot of ϵ vs %B(DAB). Three zones of different experimental accessibility can be identified; see text for details.

must be added very slowly. The drug concentration was 0.02 mM (solution B). Drugs were in all cases solubilized by adding 5% DMSO.

Four milliliters of A and 4 mL of B were transferred to centrifuge tubes and mixed for at least 4 h (solution C). The final concentration of drug and of albumin in C was one-half the initial value (0.3 and 0.01, respectively). C was centrifuged for 15 h at 34000 rpm at 10 °C in a Beckman L8-50M/E Class H Ultracentrifuge (Beckman Coulter, Milan, Italy) equipped with a Swing-Out Rotor TST 41.14 (Centrikon, Milan, Italy). The controls were also centrifuged to check for BSA precipitation and drug sedimentation.

One milliliter was taken from the uppermost protein-free layer, and the concentration of unbound drug was determined photometrically using the calibration plot. UV spectroscopy is less sensitive than radiolabeling assays, but at the preliminary stage of drug discovery, it is not justifiable to handle radiolabeled compounds.

The percentage of bound fraction of drug [%B(DAB)] was calculated by eq 10[50]

$$\%\mathrm{B(DAB)} = \left[\frac{(C_0 - C)}{C_0}\right] \times 100 \qquad (10)$$

where C_0 is half the concentration of solution B and C is the concentration of free drug obtained from the calibration plot after ultracentrifugation. The controls were checked to detect %BSA precipitated in the absence of the sample. Experiments in which precipitated %BSA was below 95% were discarded. UV measurement was done with a Shimadzu UV-2501PC spectrophotometer with quartz cuvettes (0.7 mL).

All experimental data and conditions were entered into a specifically prepared spreadsheet and %B(DAB) ± SD was calculated by an automated procedure. Five determinations required about 24 h of noncontinuous work.

Data accuracy depends on the UV absorption region and on the quantity of solute to detect. SD was small when two conditions were met as follows: (i) large ϵ at λ above 300 nm and (ii) drug decrease as compared with the mother solution between 20 and 80%. Figure 11 plots the coefficient of molar extinction (ϵ) vs %B(DAB); three zones representing different levels of experimental accessibility may be distinguished: zone I, great difficulty; zone II, average difficulty; and zone III, little difficulty.

Validation. Because of difficulties encountered in comparing binding data from different laboratories (mainly variations in protein nature and concentration and drug concentration), the method was validated on two compounds of different electrical natures (tenoxicam = acid; nicardipine = neutral) for which reliable binding data coupled with a clear and complete description of experimental conditions are reported in the literature (Table 3).

The physicochemical and structural properties of tenoxicam have been reported in Tsai et al.;[28] it is present as an anion at pH 7.4 and is an ideal standard because of the presence of a strong chromophore, which facilitates UV reading.[51] Dialysis experiments (see Table 3) determined the %B(DAB) to be 29.

Table 3. Method Validation: The Case of Tenoxicam

	method	%B(DAB) ± SD[a]	D (mM)[b]	BSA (mM)[c]	BSA/D[d]
	dialysis[e]	29 ± 3	0.2	0.06	0.3
I	ultracentrifugation	30 ± 1.4	0.2	0.06	0.3
II	ultracentrifugation	60 ± 0.1	2.0	0.6	0.3
III	ultracentrifugation	90 ± 1	0.02	0.6	30

[a] Tenoxicam bound percentage calculated from eq 2. [b] Tenoxicam mother solution concentration. [c] BSA mother solution concentration. [d] Ratio between BSA and tenoxicam concentration. [e] Personal communication from Dr. Pierre-Alain Carrupt, University of Lausanne (CH).

Three ultracentrifugation experiments were performed using (I) exactly the same experimental conditions, (II) the same BSA/drug ratio with physiological BSA concentration, and (III) our conditions. The results are reported in Table 3.

Nicardipine binding to various plasma proteins has been reported in Urien et al.[16] The experiments were conducted by dialysis using the radiolabeled compound. From the reported[16] K_A and n_A values, the experimental hyperbolic curve was simulated; the %B(DAB) was determined to be 97 at our conditions, which is in good agreement with 93 found by ultracentrifugation.

Influence of Ultracentrifugation Conditions. Time and temperature were selected in order to avoid tube damage. However, for amlodipine, a few tests were performed at 25 °C but no marked variation in %B(DAB) was noted.

Concentration Gradient. BSA is easier to separate than whole serum because the absence of lipoprotein enables more of the supernatant to be used.[52] However, gradient tests were performed using amlodipine as a reference compound. After centrifugation, the solution was removed in fractions of 1 mL beginning from the top and the %B(DAB) of each aliquot was determined: first aliquot, 64.6%; second aliquot, 63.5%; and third aliquot, 37.8%. All of the experiments were thus quantified using the upper fraction of the solution.

Influence of MW on Drug Sedimentation. A major drawback of ultracentifugation is drug sedimentation. To check whether this occurred in our experimental conditions, a quinidine solution was transferred to tubes and centrifuged for 15 h at 34000 rpm at 10 °C. One milliliter was taken from the uppermost solution, and the drug concentration was determined photometrically. The concentration of quinidine was the same as before centrifugation.

Ester Stability. It has recently[53] been suggested that the supposed esterase-like activity of HSA might be due to cholinesterase contamination. Although no corresponding effect has yet been found for BSA (and in Urien et al.,[16] no degradation phenomena are mentioned for nicardipine), we also tested the stability of 1,4-DHPs. In particular, the stability of amlodipine in human serum and in a BSA solution was monitored for 24 h at 37 °C.

Ionization and Lipophilicity Data. Ionization and lipophilicity data were obtained by the following general strategy: for all compounds belonging to the data sets, experimental pK_a and lipophilicity values were first sought in the literature and then checked for their reliability by comparison with standard calculation tools (see below); either in the case of missing data or doubtful values, potentiometric measurements were made. For methotrexate and tetracycline, no additional experiment was made because an in-depth analysis of their complex ionization and lipophilicity profiles is beyond the scope of this study.

pH Metric Approach to Measure pK_a and log $D^{7.4}$. For amlodipine, nicardipine, prazosin, ranitidine, and naproxen, pK_a and log $D^{7.4}$ were obtained by the pH metric technique using a GlpK_a apparatus[54] (Sirius Analytical Instruments Ltd., Forrest Row, East Sussex, United Kingdom) as described in detail elsewhere.[35,55−57]

Ionization constants were determined in the presence of methanol as cosolvent following Caron et al.[54] Aqueous pK_a values were obtained by extrapolation using the Yasuda−Shedlovsky procedure.[58]

To obtain lipophilicity data, at least four separate titrations were performed on each compound, on approximately 0.5 mM, containing various volumes of octan-1-ol (from 0.5 mL of organic solvent/20 mL of H_2O to 13 mL of organic solvent/7 mL of H_2O), in the pH range 1.8−12. The titrations were carried out under N_2 at 25.0 ± 0.1 °C. The final data were obtained by the Multiset approach, as described elsewhere.[55,56]

Calculation of pK_a and log $D^{7.4}$. To check the validity of the experimental data reported in the literature, pK_a values were calculated using ADME Boxes software.[32] For those compounds for which experimental log P^N (log P of the neutral form of the compound) values were found in the literature (see below), log $D^{7.4}$ values were calculated by applying the following procedure: the experimental log P^N was compared with the log P^N value calculated with various algorithms (ALOGP, IAlogP, CLOGP, KOWWIN, and XLOGP, available on-line at http://146.107.217.178/lab/alogps/); if the agreement between experimental and calculated values was good (this occurred for all compounds), log P^N was used to calculate log $D^{7.4}$ by eq 11 (the version given is that for bases) assuming that log P^I = log P^N − 3.[22,35]

$$D = P^N \cdot \left(\frac{1}{1 + 10^{pK_a - pH}}\right) + P^I \cdot \left(\frac{10^{pK_a - pH}}{1 + 10^{pK_a - pH}}\right) \quad (11)$$

The experimental log P^N found in the literature and used to obtain log D (see above) had to satisfy one of the following criteria: (i) obtained by potentiometry or (ii) stored as log P* in the Pomona database (Leo at http://www.daylight.com/release/index.html reports that log P* is the preferred value for measured partition coefficient).

Amlodipine Conformational Analysis. The conformational hypersurface of cationic amlodipine in a vacuum was explored by QMD as described elsewhere.[54,59] Six different geometries were chosen as starting points. QMD applied to amlodipine produced 59 conformers (ranging from 50 to 60). As a general rule, it was assumed that a conformer could exist if its difference in energy with the most stable conformer was below 10 kcal/mol. Using this assumption, 15 conformers out of 59 were retained for investigation.

Docking Strategies. Protein Preparation. The crystal structure of HSA complexed with propofol was obtained from the Protein Data Bank (entry 1e7a).[60] In the original crystal structure, two chains were present (A and B), and analysis was performed on the A chain.

In the crystal structures obtained through the PDB, the first four and the last three residues of the sequence were missing. A further 32 residues had missing atoms. Residues with missing atoms were completed using standard geometries, the residue Ser5 at the beginning of the chain was terminated with a neutral amino group, and the residue Ala578 was terminated with a carboxylate group. The orientation of the residue chains was established using the MOE rotamer[24] explorer utility. The utility generates side chain conformations by systematically rotating bonds in a side chain by discrete increments. The lowest energy conformation was chosen. All of these residues are distant from the cavity where propofol binds and, thus, do not influence the results of the docking procedure. Water molecules in the proximity of propofol were ignored because they were oriented toward the channel exit.

Stepwise Docking Procedure. A modified MOE-Dock module, kindly provided by Chemical Computing Group, was used to perform an automatic docking exploration for different positions and orientations. A genetic algorithm search procedure was used with MOE default parameters (1500 generations per run, three mutation frequencies, seven birth rates). The ligand flexibility was taken into account, and a random initial orientation was used. The final geometries were sorted using an energy criterion, and orientations within 5 kcal/mol of the minimum value were minimized with the procedure described below. We did not consider the other high energy conformers because visual inspection revealed poor superposition over the crystallographic model.

Minimization Procedure. Energy calculations were performed using the MMFF94 force field[61] implemented in MOE. The choice of this force field also gave a correct geometry for the ligand. Energy minimization was carried out following a stepwise procedure: (i) geometry optimization of all hydrogen atoms while keeping the rest of the structure fixed; (ii) geometry optimization of hydrogen and side chain atoms while keeping the backbone atoms fixed; (iii) geometry optimization of all atoms except Cα carbons; (iv) geometry optimization of protein areas with energy gradient components greater than 1 kcal mol^{-1} Å^{-1}; and (v) full geometry optimization without constraints. Electrostatic interactions were treated with a distant-dependent dielectric constant 4ϵ, as has been suggested by Christensen et al.[62]

Analysis of Results. The docking results were analyzed by using a combination of MOE tools. An empirical scoring tool was first applied to evaluate the strength of the HBs and salt bridges.[63] Each HB contact shown in the MOE window has a label attached to it, e.g., 90%, 2.9 A. This indicates HB at 90% strength and a distance of 2.9 Å. The strength of a contact is given relative to an "ideal" HB of that type, as computed by the scoring function.

The Contact Statistics application was then used to determine the preferred locations of the ligand atoms. The Contact Statistics application calculates, from the 3D atomic coordinates of a protein, preferred locations for hydrophobic and hydrophilic ligand atoms.[64,65] In MOE, the preferred locations of bound atoms are estimated from a collection of all crystallographic structures in the PDB with a resolution of 2.0 Å.[66]

The Contact Statistics application produces two preference maps: (i) a green surface, which is a 90% probability isocontour for the hydrophobic atoms, and (ii) a red surface, which is a 90% probability isocontour for the polar atoms. This means that a ligand fits the maps well if its hydrophobic atoms are located in proximity to the green surfaces and its polar atoms are located in proximity to the red surfaces. When the ligand matches the preference maps well, a good interaction is expected. SIMCA software[67] was used to perform PCA and XLSTAT[68] to run linear and multilinear regressions. All molecular modeling manipulations and calculations were performed using MOE, Version 2002.03, software available from Chemical Computing Group Inc., 1010 Sherbrooke Street West, Suite 910, Montreal, Canada H3A 2R7; http://www.chemcomp.com.

Acknowledgment. We thank Sirius Analytical Instruments Ltd. (Forest Row, United Kingdom) for donating the copy of Absolv software used for this research, Dr. Rosella Casullo for helpful discussions, and Prof. Bernard Testa for his help in revising the manuscript. G.E. and G.C. are indebted to the University of Turin for financial support.

References

(1) Seydel, J. K. Quantitative structure-pharmacokinetics relationships and their importance in drug design, possibilities and limitations. *Methods Find. Exp. Clin. Pharmacol.* **1984**, *6*, 571−581.

(2) Urien, S.; Tillement, J. P.; Barré, J. The significance of plasma-protein binding in drug research. In *Pharmacokinetic Optimization in Drug Research*; Testa, B., van de Waterbeemd, H., Folkers, G., Guy, R. H., Eds.; Wiley-VCH: Zürich, 2001; pp 189−197.

(3) van de Waterbeemd, H.; Smith, D. A.; Beaumont, K.; Walker, D. K. Property-based design: Optimization of drug absorption and pharmacokinetics. *J. Med. Chem.* **2001**, *44*, 1313−1333.

(4) Bhattacharya, A. A.; Grüne, T.; Curry, S. Chrystallographic analysis reveals common modes of binding of medium and long-chain fatty acids to human serum albumin. *J. Mol. Biol.* **2000**, *303*, 721−732.

(5) Petitpas, I.; Grüne, T.; Bhattacharya, A. A.; Curry, S. Crystal structures of human serum albumin complexed with monounsaturated and polyunsatured fatty acid. *J. Mol. Biol.* **2001**, *314*, 955−960.

(6) Petitpas, I.; Bhattacharya, A. A.; Twine, S.; East, M.; Curry, S. Crystal structure analysis of warfarin binding to human serum albumin. *J. Biol. Chem.* **2001**, *276*, 22804−22809.

(7) Bhattacharya, A. A.; Curry, S.; Franks, P. Binding of the general anesthetic propofol and halothane to human serum albumin. *J. Biol. Chem.* **2000**, *275*, 38731−38738.
(8) Colmenarejo, G.; Alvarez-Pedraglio, A.; Lavandera, J.-L. Cheminformatic models to predict binding affinities to human serum albumin. *J. Med. Chem.* **2001**, *44*, 4370−4378.
(9) Kratochwil, N. A.; Huber, W.; Müller, F.; Kansy, M.; Gerber, P. R. Predicting plasma protein binding of drugs: a new approach. *Biochem. Pharmacol.* **2002**, *64*, 1355−1374.
(10) Vallner, J. J. Binding of drugs by albumin and plasma protein. *J. Pharm. Sci.* **1977**, *66*, 447−465.
(11) Cserhati, T.; Forgacs, E.; Deyl, Z.; Miksik, I. Effect of molecular parameters on the binding of phenoxyacetic acid derivatives to albumin. *J. Chromatogr. B* **2001**, *753*, 87−92.
(12) Sowell, J.; Christian Mason, J.; Strekowski, L.; Patonay, G. Binding constant determination of drugs toward subdomain IIIA of human serum albumin by near-infrared dye-displacement capillary electrophoresis. *Electrophoresis* **2001**, *22*, 2512−2517.
(13) Seydel, J. K.; Butte, W. *p*-Aminobenzoic acid derivatives. Mode of action and structure−activity relationships in cell-free system (*Escherichia coli*). *J. Med. Chem.* **1977**, *20*, 439−447.
(14) Seydel, J. K.; Trettin, D.; Cordes, H. P.; Wassermann, O.; Malyusz, M. Quantitative structure−pharmacokinetic relationships derived on antibacterial sulfonamides in rats and its comparison to quantitative structure−activity relationships. *J. Med. Chem.* **1980**, *23*, 607−613.
(15) Girard, I.; Ferry, S. Protein binding of methohexital. Study of parameters modulating factors using the equilibrium dialysis technique. *J. Pharm. Biomed. Anal.* **1996**, *14*, 583−591.
(16) Urien, S.; Albengres, E.; Comte, A.; Kiechel, J.-R.; Tillement, J. P. Plasma protein binding and erythrocite partitioning of nicardipine in vitro. *J. Cardiovasc. Pharmacol.* **1985**, *7*, 891−898.
(17) Silva, C.; Plazzi, P. V.; Bordi, F.; Rivara, S.; Vacondio, F.; Zuliani, V.; Caretta, A.; Mor, M. Structure−property relationships on histamine H3-antagonists: Binding of phenyl-substituted alkylthioimidazole derivatives to rat plasma proteins. *Farmaco* **2000**, *55*, 239−245.
(18) Hervé, F.; Caron, G. Ligand specificity of the genetic variants of human α1-acid glycoprotein: generation of a three-dimensional quantitative structure−activity relationship model for drug binding to the A variant. *Mol. Pharmacol.* **1998**, *54*, 129−138.
(19) Peters, T. P. *All About Albumin. Biochemistry, Genetics, and Medical Applications*; Academic Press: New York, 1995.
(20) Matsushita, Y.; Moriguchi, I. Measurement of protein binding by ultracentrifugation. *Chem. Pharm. Bull.* **2003**, *33*, 2948−2955.
(21) Testa, B.; Crivori, P.; Reist, M.; Carrupt, P. A. *The Influence of Lipophilicity on the Pharmacokinetic Behavior of Drugs: Concepts and Examples*; Kluwer Academic Publisher: Norwell, MA, 2000; pp 179−211.
(22) Caron, G.; Reymond, F.; Carrupt, P. A.; Girault, H. H.; Testa, B. Combined molecular lipophilicity descriptors and their role in understanding intramolecular effects. *PSST* **1999**, *2*, 327−335.
(23) Berman, H. M.; Westbrook, J.; Feng, Z.; Gilliland, G.; Bhat, T. N.; Weissig, H.; Shindyalov, I. N.; Bourne, P. E. The protein data bank. *Nucleic Acids Res.* **2000**, *28*, 235.
(24) *MOE, 2002.03*; Chemical Computing Group Inc: Montreal, Quebec Canada, 2002.
(25) Bergström, C. A. S.; Strafford, M.; Lazorova, L.; Avdeef, A.; Luthman, K.; Artursson, P. Absorption classification of oral drugs based on molecular surface properties. *J. Med. Chem.* **2003**, *46*, 558−570.
(26) Taira, Z.; Terada, H. Specific and nonspecific ligand binding to serum albumin. *Biochem. Pharmacol.* **1985**, *34*, 1999−2005.
(27) Joseph-McCarthy, D. Computational approaches to structure-based ligand design. *Pharmacol. Ther.* **1999**, *84*, 179−191.
(28) Tsai, R. S.; Carrupt, P. A.; El Tayar, N.; Testa, B.; Giroud, Y.; Andrade, P.; Brée, F.; Tillement, J. P. Physicochemical and structural properties of nonsteroidal antiinflammatory oxicams. *Helv. Chim. Acta* **1993**, *76*, 842−854.
(29) Pagliara, A.; Carrupt, P. A.; Caron, G.; Gaillard, P.; Testa, B. Lipophilicity profiles of ampholytes. *Chem. Rev.* **1997**, *97*, 3385−3400.
(30) Colaizzi, J. L.; Klink, P. R. pH-Partition Behavior of Tetracyclines. *J. Pharm. Sci.* **1969**, *58*, 1184−1189.
(31) Abraham, M. H. Hydrogen bonding. 27. Solvation parameters for functionally substituted aromatic compounds and heterocyclic compounds, from gas−liquid chromatography data. *J. Chromatogr.* **1993**, *644*, 95−139.
(32) *ADME Boxes*; Advanced Pharma Algorithms: Toronto, Canada, 2003.
(33) Newton, D. W.; Kluza, R. B. pK_a values of medicinal compounds in pharmacy practice. *Drug Intell. Clin. Pharm.* **1978**, *12*, 546−554.
(34) Reymond, F.; Gobry, V.; Bouchard, G.; Girault, H. H. Electrochemical aspects of drug partitioning. In *Pharmacokinetic Optimization in Drug Research*; Testa, B., van de Waterbeemd, H., Folkers, G., Guy, R. H., Eds.; VHCA: Zürich, 2001; pp 327−349.
(35) Comer, J. E.; Tam, K. Y. Lipophilicity profiles: Theory and measurement. In *Pharmacokinetic Optimization in Drug Research*; Testa, B., van de Waterbeemd, H., Folkers, G., Guy, R. H., Eds.; Wiley-VCH: Zürich, 2001; pp 275−304.
(36) Bouchard, G.; Carrupt, P. A.; Testa, B.; Gobry, V.; Girault, H. H. Lipophilicity and solvation of anionic drugs. *Chem. Eur. J.* **2002**, *8*, 3478−3484.
(37) Plempler van Balen, G.; a Marca Martinet, C.; Caron, G.; Bouchard, G.; Reist, M.; Carrupt, P. A.; Fruttero, R.; Gasco, A.; Testa, B. Liposomes/water lipophilicity: Methods, information content, and pharmaceutical applications. *Med. Res. Rev.* **2004**, *24*, 299−324.
(38) Tetko, I. V.; Tanchuk, V. Y.; Kasheva, T. N.; Villa, A. E. P. Internet software for the calculation of the lipophilicity and aqueous solubility of chemical compounds. *J. Chem. Inf. Comput. Sci.* **2001**, *41*, 246−252.
(39) Tillement, J. P.; Houin, G.; Zini, R.; Urien, S.; Albengres, E.; Barré, J.; Lecomte, M.; d'Athis, P.; Sebille, B. The binding of drugs to blood plasma macromolecules: Recent advances and therapeutic significance. Academic Press: London, 1984; Vol. 13, pp 59−94.
(40) Saiakhov, R. D.; Stefan, L. R.; Klopman, G. Multiple computer-automated structure evaluation model of the plasma protein binding affinity of diverse drugs. *Perspect. Drug Discovery Des.* **2000**, *19*, 133−155.
(41) Testa, B.; Caron, G.; Crivori, P.; Rey, S.; Reist, M.; Carrupt, P. A. Lipophilicity and related molecular properties as determinants of pharmacokinetic behaviour. *Chimia* **2000**, *54*, 672−677.
(42) Fischer, M. J. E.; Bos, O. J. M.; van der Linden, R. F.; Wilting, J.; Janssen, L. H. M. Steroid binding to human serum albumin and fragments thereof. *Biochem. Pharmacol.* **1993**, *45*, 2411−2416.
(43) Melten, J. W.; Witterbrood, A. J.; Wemer, J.; Faber, D. B. On the modulating effects of temperature, albumin, pH and calcium on the free fractions of phenobarbitone and phenytoin. *J. Pharm. Pharmacol.* **1986**, *38*, 643−646.
(44) Weder, H. J.; Bickel, M. H. Interactions of drugs with proteins I: Binding of tricyclic thymoleptics to human and bovine plasma proteins. *J. Pharm. Sci.* **1970**, *59*, 1505−1507.
(45) Arrowsmith, J. E.; Campbell, S. F.; Cross, P. E.; Stubbs, J. K.; Burges, R. A.; Gardiner, D. G.; Blackburn, K. J. Long-acting dihydripyridine calcium antagonists. 1. 2-Alkoxymethyl derivatives incorporating basic substituents. *J. Med. Chem.* **1986**, *29*, 1696−1702.
(46) Taillardat-Bertschinger, A.; a Marca Martinet, C.; Carrupt, P. A.; Reist, M.; Caron, G.; Fruttero, R.; Testa, B. Molecular factors influencing retention on immobilised artificial membranes (IAM) compared to partitioning in liposomes and *n*-octanol. *Pharm. Res.* **2001**, *19*, 729−737.
(47) *Absolv*; Sirius Analytical Instruments Ltd.: Forest Row, United Kingdom, 1.4.05.63, 2000.
(48) Abraham, M. H.; Ibrahim, A.; Zissimos, A. M.; Zhao, Y. H.; Comer, J. E.; Reynolds, D. Application of hydrogen bonding calculations in property based drug design. *DDT* **2002**, *7*, 1056−1063.
(49) *Dragon, v. 3.1*; Talete Srl: Milano, Italy, 2003.
(50) Reidenberg, M. M., Erill, S., Eds. *Drug−Protein Binding*; Praeger Publishers: New York, 1986.
(51) Avdeef, A. High-throughput measurement of permeability profiles. In *Drug Bioavailability*; van de Waterbeend, H., Lennernas, H., Artursson, P., Eds.; Wiley-VCH: Weinheim, 2003; pp 46−71.
(52) Kurz, H.; Trunk, H.; Weitz, B. Evaluation of methods to determine protein-binding of drugs. *Arzneim.-Forsch.* **1977**, *27*, 1373−1380.
(53) Chapuis, N.; Brühlmann, C.; Reist, M.; Carrupt, P. A.; Mayer, J. M.; Testa, B. The esterase-like activity of serum albumin may be due to cholinesterase contamination. *Pharm. Res.* **2001**, *18*, 1435−1439.
(54) Caron, G.; Gaillard, P.; Carrupt, P. A.; Testa, B. Lipophilicity behavior of model and medicinal compounds containing a sulfide, sulfoxide, or sulfone moiety. *Helv. Chim. Acta* **1997**, *80*, 449−462.
(55) Avdeef, A. pH-Metric log P. Part 1. Difference plots for determining ion-pair octanol−water partition coefficients of multiprotic substances. *Quant. Struct.-Act. Relat.* **1992**, *11*, 510−517.
(56) Avdeef, A. pH-Metric log P. II. Refinement of partition coefficients and ionization constants of multiprotic substances. *J. Pharm. Sci.* **1993**, *82*, 183−190.
(57) Avdeef, A. Assessment of distribution-pH profiles. In *Lipophilicity in Drug Action and Toxicology*; Pliska, V., Testa, B., van de Waterbeemd, H., Eds.; VCH Publishers: Weinheim, 1996; pp 109−139.

(58) Avdeef, A.; Comer, J. E. A.; Thomson, S. J.; pH-Metric log P. 3. Glass electrode calibration in methanol−water, applied to pK_a determination of water-insoluble substances. *Anal. Chem.* **1993**, *65*, 42−49.
(59) Ermondi, G.; Caron, G.; Bouchard, G.; Plemper van Balen, G.; Pagliara, A.; Grandi, T.; Carrupt, P. A.; Fruttero, R.; Testa, B. Molecular dynamics and NMR exploration of the property space of the zwitterionic antihistamine cetirizine. *Helv. Chim. Acta* **1999**, *84*, 360−374.
(60) Bernstein, F. C.; Koetzle, T. F.; Williams, G. J.; Meyer, E. E., Jr.; Brice, M. D.; Rodgers, J. R.; Kennard, O.; Shimanouchi, T.; Tasumi, M. The protein data bank: A computer-based archival file for macromolecular structures. *J. Mol. Biol.* **1977**, *112*, 535−542.
(61) Halgren, T. A. Merck molecular force field. 1. Basis, form, scope, parametrization, and performance of MMFF94. *J. Comput. Chem.* **1996**, *17*, 490−519.
(62) Christensen, I. T.; Jorgensen, F. S. Molecular mechanics calculations of proteins. Comparison of different energy minimization strategies. *J. Biomol. Struct. Dyn.* **1997**, *15*, 473−488.
(63) *MOE 2003.02 User Guide*; Chemical Computing Group, Inc.: Montreal, Quebec, Canada, 2003.
(64) Muegge, I.; Martin, Y. C. A general and fast scoring function for protein−ligand interactions: A simplified potential approach. *J. Med. Chem.* **1999**, *42*, 791−804.
(65) Bruno, I. J.; Cole, J. C.; Lommerse, J. P. M.; Rowland, R. S.; Taylor, R.; Verdonk, M. L. IsoStar: A library of information about nonbonded interactions. *J. Comput.-Aided Mol. Des.* **1997**, *11*, 525−537.
(66) Labute, P. Probabilistic receptor potentials. *J. Chem. Comput. Group* **2003**, http://www.chemcomp.com/Journal_of_CCG/Features/cstat.htm.
(67) *SIMCA-P*, v. 10.0.2.0; Umetrics: Umea, Sweden, 2003.
(68) *XLSTAT, Data Analysis Solution for Microsoft Excel*, v. 7.1; Addinsoft: Paris, France, 2004.
(69) *Medchem95 Database*; Daylight Chemical Information System, Inc.: Irvine, California, 1995.
(70) Plemper van Balen, G.; Carrupt, P. A.; Morin, D.; Tillement, J. P.; Le Ridant, A.; Testa, B. Recognition forces involved in mitochondrial binding to a low-affinity trimetazidine binding site related to anti-ischemic activity. *Biochem. Pharmacol.* **2002**, *63*, 1691−1697.
(71) Avdeef, A. *Absorption and Drug Development. Solubility, Permeability, and Charge State*; John Wiley & Sons: New York, 2003.
(72) Auffinger, P.; Wipff, G. High-temperature annealed molecular dynamics simulations as a tool for conformational sampling—Application to the bicyclic-222 cryptand. *J. Comput. Chem.* **1990**, *11*, 19−31.
(73) Murdock, D.; Heel, R. C. Amlodipine. A review of its pharmacodynamic and pharmacokinetic properties, and therapeutic use in cardiovascular disease. *Drugs* **1991**, *41*, 478−505.
(74) Sorkin, E. M.; Clissold, S. P. Nicardipine. A review of its pharmacodynamic and pharmacokinetic properties, and therapeutic efficacy, in the treatment of angina pectoris, hypertension and related cardiovascular disorders. *Drugs* **1987**, *33*, 296−345.
(75) Jolliet, P.; Simon, N.; Brée, F.; Urien, S.; Pagliara, A.; Carrupt, P. A.; Testa, B.; Tillement, J. P. Blood-to-brain transfer of various oxicams: effects of plasma binding on their brain delivery. *Pharm. Res.* **1997**, *14*, 650−656.

JM040760A